Leveraging large-eddy simulations to investigate the influence of temperature non-uniformity on jet noise

By P. Tamm†, G. A. Brès‡, A. Towne AND S. K. Lele

Heated over-expanded supersonic jets issued from a military-style faceted converging-diverging nozzle are studied through large eddy simulations (LES). Three different flow temperature conditions are examined: a baseline, an elevated, and a non-uniform inlet profile. The near and acoustic fields of each jet are interrogated to determine the impact of temperature on the flowfield and acoustic signature. The baseline simulation is compared to experimental data for validation, and the others are run to test the utility of a non-uniform temperature profile for noise mitigation. The preliminary results from the simulation of the non-uniform temperature profile indicate a reduction in the noise output of the jet, both in overall peak levels and radiated power, independent of performance losses.

1. Introduction

The flight deck of an aircraft carrier is one of the world's loudest environments, due to the plethora of jet-propelled aircraft in close quarters. Flight deck operations involve several flight crew personnel working in close proximity to these aircraft, leading to the potential for significant hearing loss later in life. When working on the flight deck, crew members are exposed to sustained noise in excess of 145 dB, requiring double hearing protection. Despite the hearing protection, the Department of Veteran's Affairs spends more than $4 billion annually on health care related to hearing loss (Aubert & McKinley 2011). The main source of the noise coming from a military aircraft is the hot stream of air being expelled from the exhaust nozzle. Variable military nozzles are designed to operate primarily at altitude, to provide the best performance during a given mission. With the exception of nozzles that are fully controlled, these nozzles have only a select few operational points, none of which are meant for takeoff, sea level conditions. The high pressure at sea level during takeoff relative to the nozzle design altitude leads the supersonic exhaust flow from the nozzle to be over-expanded. This non-ideal expansion of the flow leads to even higher noise levels, as the flow develops shocks as it is decelerated while raising its pressure to match the ambient.

For many years, the problem of aircraft noise was not unique to military operations. The commercial aviation industry has had to deal with aircraft noise generated at airports, which had been an aggravation to local residents. As commercial engines operate entirely in subsonic flight, their large bypass ratios lend themselves to certain easily implemented methods of noise reduction. Adding chevrons to the aft end of the nacelle is a large and wide-ranging success on commercial engines. The chevrons disrupt the stream

† US Navy, Naval Air Systems Command
‡ Cascade Technologies, Inc.

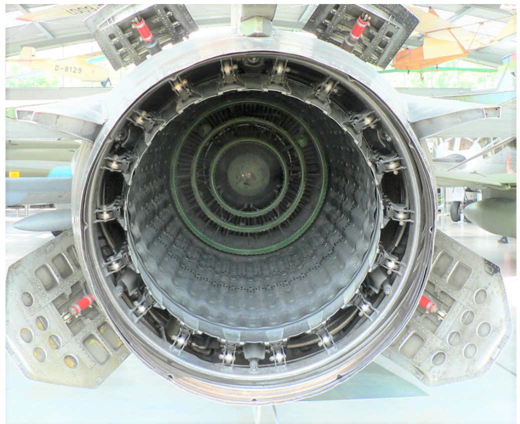

FIGURE 1: Afterburner configuration of a MiG-23. There are three rings of flameholders, with the aft end of the engine centerbody in the middle.

of the bypass, introducing vorticity to smooth the mixing of hot and cold jets (Bridges *et al.* 2011), and break the axisymmetric nature of the jet.

While chevrons work well for the commercial industry, they are not currently leveraged for use on fighter jets. Chevrons reduce the performance of the engine, and unless they are actuated as well, chevrons will be perpetually perturbing the exhaust flow, even at altitude, where noise reduction is not needed. Actuating the chevrons would add weight and complexity to the aircraft, ultimately driving up the cost. The limitation of having little to no impact on the engine performance, especially during the mission, is a primary driver of the design process for investigating these solutions. One potential method for overcoming this problem of noise without greatly impacting the engine performance has been proposed by Mayo *et al.* (2017). This method involves the injection of cold flow along the centerline of the nozzle. The underlying principle of creating a non-uniform temperature profile would apply to an annular afterburner configuration similar to what is shown in Figure 1, which is looking up the exhaust nozzle of a MiG-23. The annular shape of the flame holders would allow a stream of normal turbine exhaust along the engine centerline by only injecting and burning extra fuel around the outer flame holding rings. The temperature disparity facilitates the growth of the shear layer and a reduction in length of the potential core.

The concept of a non-uniform temperature profile has been experimentally investigated at relatively low temperature ratios using near-field particle image velocimetry (PIV) and acoustic measurements. Performing experiments at higher, more realistic temperature ratios is challenging due to physical limitations and would likely require costly facility upgrades. Moreover, limited measurements are possible in an experimental setting. On the other hand, large eddy simulation (LES) is not constrained in this way and can be used to study the flow at realistic engine operating temperatures, at all locations within a fully 3-D volume.

In this paper, we use LES to investigate the impact of temperature non-uniformity on the noise generated by over-expanded supersonic jets. We begin in Section 2 by describing the physical setup and the simulation methodology. Validations of the simulations and the impact of the non-uniform temperature profile are broken down in Section 3. Finally, the work is summarized in Section 4.

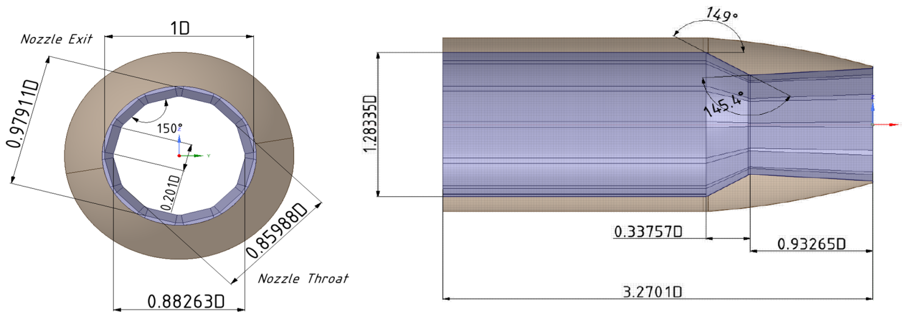

(a) (b)

FIGURE 2: Nozzle dimensions: (a) cross section, (b) streamwise section.

2. Methods

This investigation examined the flow through a GE F404 like nozzle that has been widely studied in academia. The nozzle is a converging-diverging faceted nozzle, with 12 large facets and 12 smaller facets connecting the larger ones. The nozzle has been thoroughly experimentally studied by many groups; the nozzle is roughly 5 inches in diameter, and additional details on the nozzle along with its dimensions can be found in Figure 2. The full experimental setup, to which the military power (baseline) simulation is compared, is detailed by Bridges *et al.* (2011). To experimentally measure farfield noise, microphones were set up in an arc with radius of about 100 nozzle diameters.

The simulations were run using the unstructured compressible flow solver CharLES (Brès *et al.* 2017) developed at Cascade Technologies, Inc. For the present version of the CharLES solver, the mesh is generated through the computation of a Voronoi diagram (Ambo *et al.* 2017; Brès *et al.* 2018,1), which drastically simplifies the meshing of complex geometry and results in high-quality, nearly isotropic grids. The fluid was assumed to be a perfect gas with specific heat ratio $\gamma = 1.4$; combustion products and effects were ignored. As laid out in Brès *et al.* (2018,2), wall-stress modeling based on the equilibrium boundary layer assumption (Larsson *et al.* 2016; Bose & Park 2018), and near-wall grid refinement are used for the interior surface of the nozzle, in the convergent, throat, and divergent sections. The most refined mesh used for each case was about 57 million cells, with emphasized refinement along the walls and within the shear layer of the jet; details such as the finer mesh just downstream of the lipline can seen in Figure 3.

The farfield noise simulation analysis was conducted by constructing Ffowcs-Williams Hawking (FW-H) surfaces (Ffowcs Williams & Hawkings 1969), which utilize the acoustic analogy to obtain the farfield noise. The current implementation of FW-H surfaces within CharLES is described by Brès *et al.* (2017). The method of endcaps as described by Shur *et al.* (2005), where farfield pressure is estimated by averaging over multiple outflow disks, was utilized. To build the LES database, a cylindrical grid of 15 million probes recorded the primitive variables (ρ, u, v, w, $p - 1/\gamma$) within the hot jet and the nearfield. The grid consists of 128 points evenly spaced azimuthally to enable the calculation of an azimuthal Fourier transform. For each case, the LES database was recorded at a constant interval of $\Delta t c_\infty / D = 0.1$ for the length of the simulation, resulting in 5000 snapshots of data.

Three separate simulations were conducted, each for a different engine operating con-

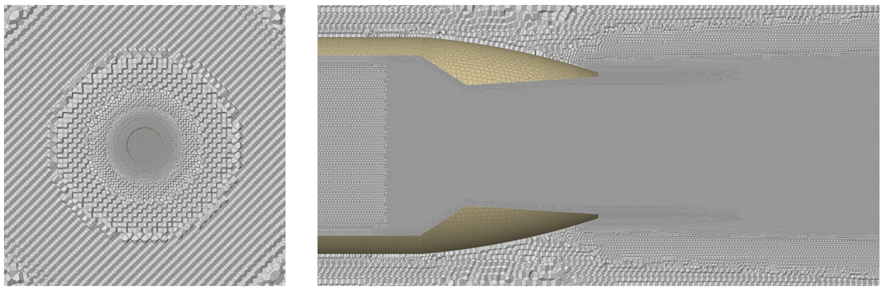

(a) (b)

FIGURE 3: Mesh details: (a) cross-stream section of mesh, at the nozzle exit plane, (b) streamwise section of mesh, cut through a large facet. Note the refinement just right of the nozzle lip.

dition: first, a flow at military power, which is used to validate the simulation process through comparison to experimental data; second, a flow at an afterburning condition which characterizes the noise increase with regard to temperature; third, a flow with the non-uniform temperature profile, consisting of an annulus of afterburned exhaust and a center stream of military power exhaust, which is compared to the afterburning condition. The spatially varying boundary condition for the non-uniform case was achieved by prescribing a hyperbolic tangent profile radially at the nozzle inlet. All three cases were run with identical geometry, to isolate the impact of temperature. Table 1 provides a breakdown of the conditions for the three cases. All three cases have the same nozzle pressure ratio (NPR), as it was assumed the added combustion occurs at constant pressure. This assumption, along with the ideal gas equation of state, leads to each case operating at a condition of equivalent thrust. While this is not a completely accurate representation of on-wing nozzle behavior, it allows for a comparison of noise levels independent of influence from thrust reductions. The varying temperature profile makes defining parameters such as the acoustic Mach number and Reynolds number of the jet difficult, so they are not listed in the table.

3. Results

3.1. *Preliminary comparison to experimental data*

The first step of the investigation was to compare the experimental data from Bridges *et al.* (2011) for the nozzle without chevrons, to the simulated case of military power. Both the flowfield and the acoustics (Henderson & Bridges 2010) were assessed. The experimental data were collected using PIV and the flowfield was interrogated in both the streamwise and cross-stream directions. A comparison of the centerline velocities can be seen in Figure 4. The dramatic shift in velocities are attributed to the shock cells within the jet as the flow progresses downstream. At times the strength of the shocks is overestimated, but the locations match well. Specifically, the shocks are overestimated farther downstream of the nozzle. The length of the potential core can be observed in the figure as well, and the associated decrease in velocity after the shock train indicates that the code matches the length quite accurately.

Figure 8 compares the overall sound pressure level (OASPL) seen by a polar array at a distance of about 100 diameters. For a blind study, the results are encouraging; the

Case name	M_d	NPR	NTR$_{core}$	NTR$_{outer}$	M_a	Re
Mil Power	1.56	3.51	2.99	2.99	2.025	2E6
Afterburner	1.56	3.51	7	7	3.096	0.7E6
Non-uniform	1.56	3.51	2.99	7	-	-

TABLE 1: Simulation parameters for each power setting. Nozzle design Mach number, nozzle pressure ratio, nozzle temperature ratio of the core and annulus, acoustic Mach number, and Reynolds number.

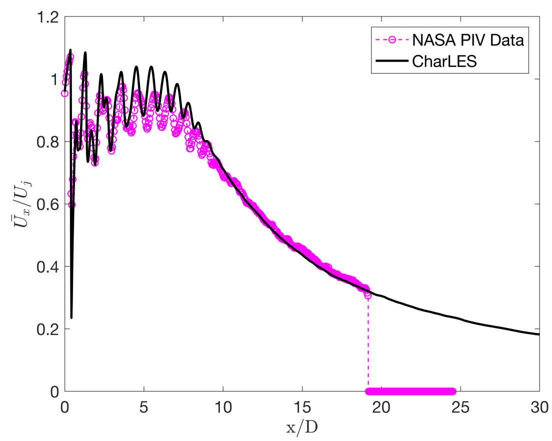

FIGURE 4: Average centerline velocity comparison.

peak directivity angle is captured, and the peak OASPL is overestimated by only a few decibels. As seen in Figure 9 for the frequency spectra at the peak directivity angle, the simulation closely matches the experimental data, over low and high frequencies, until the simulation drops off at the highest end of the range.

3.2. *Afterburning cases*

With regard to the afterburner and non-uniform temperature cases, the increased temperature of the flow, but equal NPR, leads to the same Mach number for all three cases. However, the actual speed of sound, and therefore the flow velocity, is different. Figure 5 provides insight on the instantaneous streamwise temperature contours of both afterburning cases. The shear layer structures are highlighted, and specifically in the case of the non-uniform profile, the interaction between the hot and cold streams can begin to be inspected. The cooler flow along the centerline persists significantly downstream of the nozzle exit before mixing out. The equal NPR results in the same shock structure, shown in Figure 6. The streamwise contours also emphasize that there is little, if any, change to the shear layer spreading angle. The introduction of the cooler flow in the non-uniform temperature profile reduces the velocity gradient within the shear layer. As the convective velocity is a known source of noise, it is immediately promising that the overall flow features are corresponding to a reduction in noise.

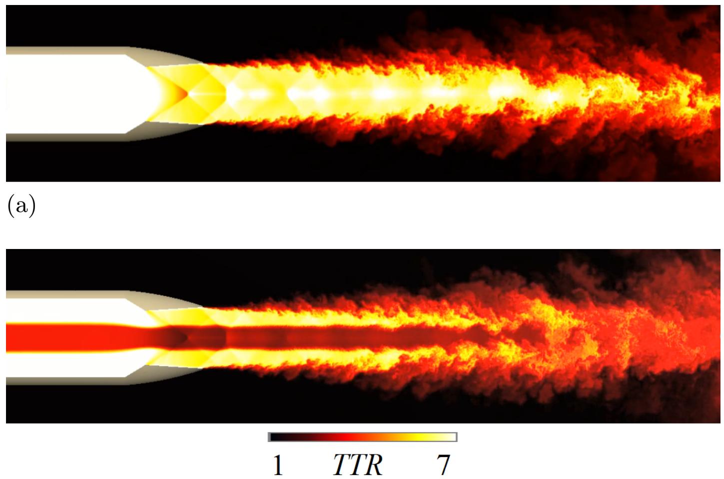

(a)

(b)

FIGURE 5: Instantaneous temperature: (a) full afterburner, (b) non-uniform temperature profile.

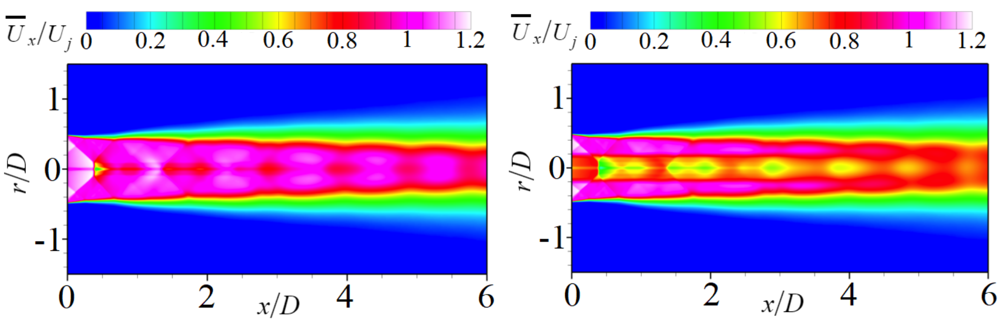

(a) (b)

FIGURE 6: Averaged streamwise velocity contours: (a) full afterburner, (b) non-uniform temperature profile.

The nozzle lipline, a line extending out in the axial direction from the nozzle lip, which can capture aspects of the shear layer, was also compared between the cases. Given that the lip has two sizes of facets, the large and small facets were averaged separately to account for azimuthal variation. The liplines of each elevated temperature case are compared in Figure 7. The lipline is particularly interesting for each of these cases because the flow is over-expanded. The jet separates from the nozzle wall just upstream of the exit before the shear layer spreads downstream of the nozzle exit. This is observed as a dip in the jet velocity along the lipline before the shear layer develops and spreads into the line. The non-uniform temperature profile sees a small dip in velocity, before the two streams mix together. This is indicative of a reduction in convective velocity, which would correspond to a decrease in noise output.

Comparing the acoustics, both cases have an expected, temperature-driven increase in OASPL. This calculation was done for the same 100 diameter arc, and the comparison

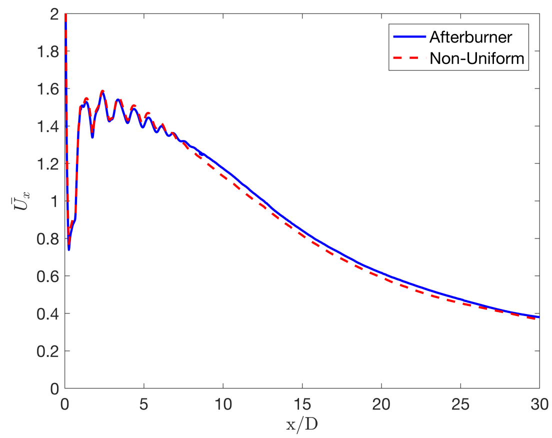

FIGURE 7: Lipline average velocity magnitude.

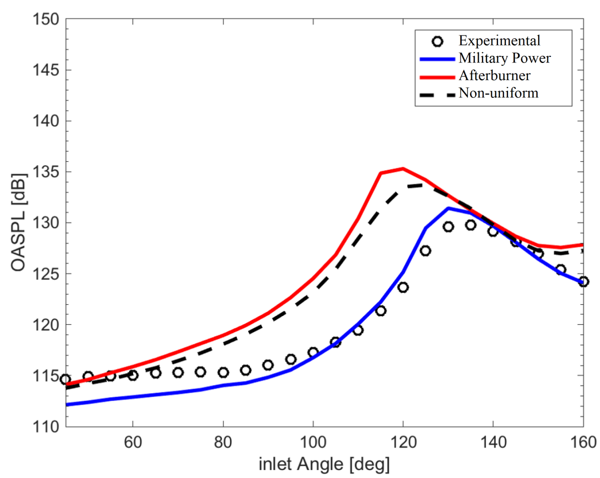

FIGURE 8: OASPL for each case.

to the military power case is also displayed in Figure 8. The non-uniform temperature case does realize a reduction of 1.6 dB in peak OASPL, along with a 1.1dB reduction in radiated power, as compared to the afterburner case. The drop in OASPL is encouraging, as well as the frequency spectra at the location, found in Figure 9. The decrease from the afterburner to the non-uniform profile is over a large frequency range. The similarities between the non-uniform temperature and afterburner in the high-frequency range indicate that the small-scale structures are not being affected. The distinct change in slope at the highest range in the plot, at about 17 kHz, corresponds to the theoretical grid cutoff, where the acoustic subgrid scale model dominates.

3.3. *Spectral proper orthogonal decomposition*

It is well known that coherent wavepacket structures within the jet play a central role in noise emissions in supersonic jets, especially in downstream directions (Jordan & Colonius 2013). To investigate the impact of temperature variations on these structures and

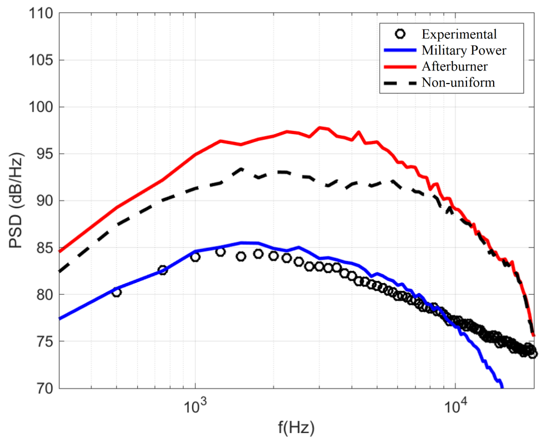

FIGURE 9: Frequency spectra for each case, at an inlet angle of 115°.

their emitted sound, the three jets were further analyzed using a frequency domain version of proper orthogonal decomposition (Lumley 1970) called spectral proper orthogonal decomposition (SPOD) (Towne *et al.* 2018). As shown by Towne *et al.* (2018), SPOD combines the advantages of the usual spatial version of POD and dynamic mode decomposition (Schmid 2010), and identifies flow structures that evolve coherently in space and time. To compute SPOD modes from our LES data, we follow the procedure outlined by Towne *et al.* (2018). To simplify the analysis, we assume azimuthal symmetry, which is not strictly true for the faceted nozzle, but we expect this to have a negligible impact on the large-scale structures of interest. (See Schmidt *et al.* (2018) for a recent application of SPOD to turbulent jets, and an example of the physical insight that can be gained from such an analysis.)

The leading SPOD mode for the axisymmetric component of the pressure field at $St = 0.63776$ for each jet is shown in Figure 10. It is clear that the temperature changes impact both the wavepackets and their associated acoustic radiation. In particular, the change in directivity angle with the increase in flow temperature that was previously observed in Figure 8 is captured by the SPOD modes, suggesting that this behavior can be related to changes in the properties of the large-scale coherent wavepacket structures. This observation will be further explored in future work using stability analysis of the jet mean flows.

4. Conclusions

LES was conducted on a faceted converging-diverging nozzle, at three operating conditions: military power, full afterburner, and non-uniform temperature inlet. The military power condition was compared to experimental data in order to validate the model and setup. The blind study of the military power case has initially compared well, exhibiting many of the same prominent flow features, along with close acoustic accuracy to experimental data. The afterburning case was then contrasted with the non-uniform temperature profile, in an effort to decrease the noise of the exhaust jet. A 1.6 dB reduction in peak OASPL and 1.1 dB reduction in radiated power were realized. The noise reduction was consistent with observed behavior of the flow. The concept of a non-uniform temperature profile had previously been investigated experimentally only at low temperatures

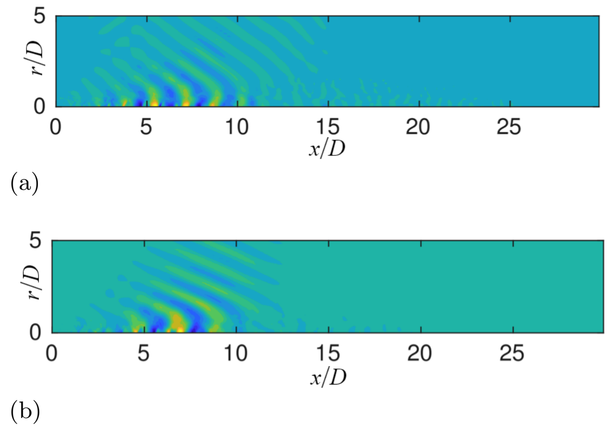

FIGURE 10: SPOD of (a) military power, (b) full afterburner.

and temperature ratios; the results of the present study indicate that there is merit to the idea when taking into consideration more realistic conditions.

Much work remains to fully analyze the three LES databases generated by this investigation. Additionally, there are ways to improve the simulations done, along with more concepts worthy of examination. The assumption of a single ideal gas with constant γ used in the current simulation will be revisited in future computations. Modeling of the combustion product properties and mixing with ambient air could potentially improve accuracy and provide further physical insight on the jet behavior in real systems. The chance to have a variable γ would also increase simulation fidelity, as the value is known not to be constant, and the impact on jet noise has been studied by Liu *et al.* (2016). Finally, there is additional work from Mayo *et al.* (2018), where the cold spot is moved to a wall, creating an asymmetric profile. The new spot location increases shear layer thickness, and a reduction in local peak shear stress levels. The disruption of the shear layer indicates a potential reduction in high-frequency noise. The breadth of follow on work, and the promising preliminary results, combine to augur many exciting ways forward with this work.

Acknowledgments

The authors acknowledge use of computational resources from the Certainty cluster awarded by the National Science Foundation to CTR. The authors would also like to acknowledge the computational resources provided by the Department of Defense High Performance Computing Modernization Program, specifically the Onyx HPC, at the DoD ERDC. Finally, the authors thank Dr. Oliver T. Schmidt for his review of an earlier draft of this report and Dr. James Bridges for providing the experimental data.

REFERENCES

AMBO, K., YOSHINO, T., KAWAMURA, T. & TERAMURA, M. 2017 Comparison between wall-modeled and wall-resolved large eddy simulations for the prediction of boundary layer separation around the side mirror of a full-scale vehicle. *AIAA Paper* 2017-1661.

Aubert, A. & McKinley, R. 2011 Measurements of jet noise aboard U.S. Navy aircraft carriers. *AIAA Paper* 2011-6947.

Bose, S. & Park, G. I. 2018 Wall-modeled large eddy simulation for complex turbulent flows. *Annu. Rev. Fluid Mech.*, **50** (1), 535–561.

Brès, G. A., Ham, F. E., Nichols, J. W., & Lele, S. K. 2017 Unstructured Large Eddy Simulations of Supersonic Jets. *AIAA J.* **55** (4), 1164–1184.

Brès, G. A., Bose, S. T., Emory, M., Ham, F. E., Schmidt, O. T., Rigas, G., & Colonius, T. 2018 Large-eddy simulations of co-annular turbulent jet using a voronoi-based mesh generation framework. *AIAA Paper* 2018-3302.

Brès, G. A., Jordan, P., Jaunet, V., Le Rallic, M., Cavalieri, A. V. G., Towne, A., Lele, S. K., Colonius, T. & Schmidt, O. T. 2018 Importance of the nozzle-exit boundary-layer state in subsonic turbulent jets. *J. Fluid Mech.* **851**, 83–124.

Bridges, J., Wernet, M., & Frate, F. 2011 PIV measurements of chevrons on F400-series tactical aircraft nozzle model. *AIAA Paper* 2011-1157.

Ffowcs Williams, J. E. & Hawkings, D. L. 1969 Sound generation by turbulence and surfaces in arbitrary motion. In *Royal Society of London Philosophical Transactions Series A*, pp. 321–342.

Henderson, B. & Bridges, J. 2010 An MDOE Investigation of Chevrons for Supersonic Jet Noise Reduction. *AIAA Paper* 2010-3926.

Jordan, P. & Colonius, T. 2013 Wave packets and turbulent jet noise. *Annu. Rev. Fluid Mech.* **45** (1), 173–195.

Larsson, J. K., S., Bodart, J. & Bermejo-Moreno, I. 2016 Large eddy simulation with modeled wall-stress: recent progress and future directions. *Mech. Eng. Rev.*, pp. 3, 15–00418.

Liu, J., Corrigan, A. T., Kailasanath, K. & Taylor, B. D. 2016 Impact of the specific heat ratio on the noise generation in a high temperature supersonic jet. *AIAA Paper* 2016-2125.

Lumley, J. L. 1970 Stochastic tools in turbulence. *J. Fluid Mech.* **67** (2), 413–415.

Mayo, D. E., Daniel, K., Lowe, K. T. & Ng, W. F. 2017 Experimental investigation of a heated supersonic jet with total temperature non-uniformity. *AIAA Paper* 2017-3521.

Mayo, D. E., Daniel, K., Lowe, T. & Ng., W. 2018 The flow and turbulance characteristics of a heated supersonic jet with an offset total temperature non-uniformity. *AIAA Paper* 2018-3144.

Schmid, P. J. 2010 Dynamic mode decomposition of numerical and experimental data. *J. Fluid Mech.* **656** (2), 5–28.

Schmidt, O. T., Towne, A., Rigas, G., Colonius, T. & Brès, G. A. 2018 Spectral analysis of jet turbulence. *J. Fluid Mech.* **855**, 953–982.

Shur, M. L., Spalart, P. R. & Strelets, M. K. 2005 Noise predictions for increasingly complex jets. part i: Methods and tests. *Int. J. Aeroacoust.* **4** (3-4), 213–246.

Towne, A., Schmidt, O. T. & Colonius, T. 2018 Spectral proper othogonal decomposition and its relationship to dynamic mode decomposition and resolvent analysis. *J. Fluid Mech.* **847**, 821–867.